

# Road Estimation and Fuel Optimal Control of an Off-Road Vehicle

Jörgen Albrektsson<sup>1,2</sup> and Jan Åslund<sup>1</sup>

<sup>1</sup>Department of Electrical Engineering, Linköping University, SE-581 83 Linköping, Sweden

<sup>2</sup>Volvo Construction Equipment, SE-631 85 Eskilstuna, Sweden

**Keywords:** Off-road, Construction Equipment, Kalman Filters, Rolling Resistance, Optimal Control, Dynamic Programming.

**Abstract:** This paper explores the possibility to use optimal control to establish a Pareto front of fuel consumption vs cycle time for a transport mission with an articulated hauler. The Pareto front can be utilised to optimise the hauler transport mission on its own or as a part in a larger optimal control problem involving several construction machines working together on a site transporting material at a set production rate. While rolling resistance is a major energy consumer in an articulated hauler's transport, the effect of varying rolling resistance is included in the developed optimisation algorithm. A method utilising Extended Kalman Filter, Rauch-Tung-Striebel smoothing and sensor fusion is formulated in order to calculate the road related data needed in the optimisation algorithm. A potential fuel efficiency improvement, verified by computer simulations, of up to 9% was found in the example transport mission where the optimal gear and speed trajectory were followed instead of driving towards a mean speed target to achieve an equal cycle time for the transport mission.

## 1 INTRODUCTION

In the construction industry today articulated haulers are used in a vast amount of different transport missions due to its ability to work efficiently even at tough (off-)road conditions. Commonly there is a set production target [ton/h] for the transport mission, i.e. the hauler should transport a certain amount of material in a set time. This work explores the possibility to use optimal control to establish a Pareto front of fuel consumption vs cycle time for a transport mission with an articulated hauler. The Pareto front can be utilised to optimise the transport mission on its own or as a part in a larger optimal control problem involving several construction machines. Predictive cruise control is today a common feature in commercial vehicles. Through calculation of an optimal vehicle speed trajectory on a priori known road stretch a reduction in fuel consumption and  $CO_2$  emissions can be achieved. The optimisation algorithm analyses the road elevation to make use of the potential energy that is released in down slopes, preserves the energy as kinetic energy in the vehicle which is then used when the road is going up again. In combination with optimising the choice of gear, enabling the internal combustion engine (ICE) to work efficiently, further fuel consumption reduction is possible. The

working conditions of an off-road vehicle differ in some respects substantially compared to an on-road vehicle. Off-road the fluctuation in elevation of the road is steeper and more frequent and the road surface is much rougher. The differences in the working environment results in a much lower average speed of an off-road vehicle compared to an on-road truck. These conditions shifts the relation between energy consumers making rolling resistance dominate over air-drag off-road compared to the opposite in a typical on-road truck application (21st Century truck partnership, 2013). In (Fu and Bortolin, 2012) the possibility of using Dynamic Programming is explored to optimise a vehicle speed trajectory and to build a gear shift strategy for an articulated hauler. This paper expands earlier research through also consider varying rolling resistance in the optimisation algorithm and to include an algorithm that estimates the rolling resistance along the track. The paper is disposed as follows: Section 2 presents a vehicle model of an articulated hauler, the model is essentially equal when applied both in the map module and optimisation algorithm. In Section 3 a method to estimate and record the road characteristics is developed. Section 4 displays a method for optimal control of the hauler and the method used to build the Pareto front. Section 5 presents results from tests and simulations.

## 2 VEHICLE MODEL

In this section the driveline and the complete vehicle are modelled. The models are used both in the map module and in the optimisation algorithm. The displayed models are the ones used in the map module while the end of the section explains the needed updates when applied in the optimisation algorithm.

### 2.1 External Forces Acting on the Hauler

There are several forces acting on a vehicle as it starts to move, see i.e. (Guzzella and Sciarretta, 2013). The main longitudinal forces acting on the articulated hauler are displayed in Figure 1.



Figure 1: Longitudinal forces acting on an articulated hauler.

In Figure 1 the following models / notation apply:

**Vehicle Speed,  $v$**

**Road Inclination,  $\alpha$**

**Tractive Force (retarding if negative),  $F_t$**

**Aerodynamic Force,  $F_a$ .** The motion of an object through the atmosphere gives rise to an aerodynamic resisting force. For a vehicle  $F_a$  is often modelled to be dependent on the density of the surrounding air,  $\rho_a$ , the front area of the vehicle,  $A_f$ , an aerodynamic drag coefficient,  $c_d$  and the velocity of the vehicle,  $v$ , in square.

$$F_a = \frac{1}{2} \rho_a \cdot A_f \cdot c_d \cdot v^2 \quad (1)$$

**Rolling Resistance Force,  $F_r$ .** The rolling resistance force can be modelled as

$$F_r = c_r \cdot m_{veh} \cdot g \cdot \cos(\alpha) \quad (2)$$

The rolling resistance coefficient,  $c_r$ , depends on many variables such as vehicle speed, tire pressure and road surface conditions. In our case the rolling resistance coefficient is one of the parameters that are estimated in the map building process and variations in these variables will indirectly affect the estimation of  $c_r$ .

**Force Generated by Road Inclination,  $F_g$ .** As the vehicle moves up-hill or down-hill the gravity will

create a retarding or accelerating force depending on the angle of the slope,  $\alpha$ . This force is modelled as

$$F_g = m_{veh} \cdot g \cdot \sin(\alpha) \quad (3)$$

### 2.2 Drivetrain Model

The drivetrain in a Volvo articulated hauler is shown in Figure 2. The main components in the hauler drivetrain are from left to right: internal combustion engine, torque converter, gear box, drop box, central gear, hub, brake and (wheel).



Figure 2: Drivetrain in a Volvo A40G Articulated hauler.

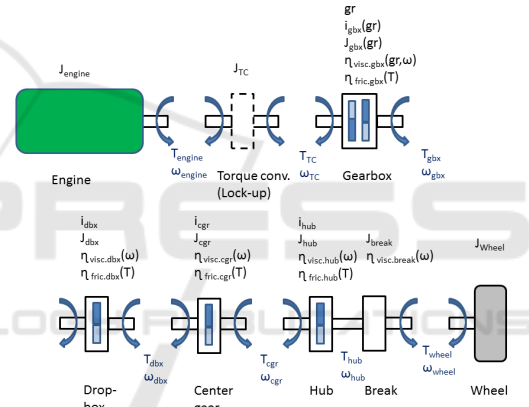


Figure 3: Drivetrain model.

Figure 3 displays how the model of the drivetrain is built. The notation used in picture 3 is:  $T$  = torque [Nm],  $\omega$  = angular velocity [rad/s],  $gr$  = gear [-],  $J$  = mass moment of inertia [  $kgm^2$  ],  $i$  = gear ratio [-],  $\eta$  = efficiency [ % ].

**Internal Combustion Engine ( ICE ).** When used in the map module the measured torque generated by the internal combustion engine is an input to the drivetrain model. The net generated torque,  $T_{engine}$ , is estimated by the engine management system (EMS) and broadcasted on the vehicle CAN network. No deeper description on how the torque is estimated by the EMS is considered to be needed at this point. Newton's second law of motion, with dots representing the time derivatives, connects angular acceleration to torque,

$$J_{engine} \cdot \dot{\omega}_{engine} = T_{engine} - T_{TC} \quad (4)$$

where  $J$  = inertia,  $\omega_{engine}$  = engine angular speed and  $T_{TC}$  is the torque at node torque converter.

**Torque Converter ( TC ).** A torque converter with lock-up functionality is bolted on the crankshaft of the ICE connecting the engine to the gear box. A Volvo A40G hauler is predominantly running in lock-up mode. Only at take-off and at very steep uphill slopes the hauler runs in torque converter mode. Thus the drivetrain model is limited to only consider lock-up mode and the TC is modelled as a stiff axle with additional inertia according to (5):

$$\begin{aligned} T_{TC} &= T_{engine} \\ \omega_{TC} &= \omega_{engine} \end{aligned} \quad (5)$$

**Gear Box ( gbx ).** The Volvo A40G is equipped with a Powertronic gear box with 9 forward gears and 4 reverse gears. The Powertronic gearbox is of planetary type and gear shifts are made by means of engaging and disengaging clutches. A major advantage with this design is that gear shifts can be performed without torque loss and the vehicle loses no kinetic energy during a gear shift. During the gear shift a change in efficiency of the gear box is likely but this is not reflected in the gear box model when used in the map module since it is judged to be of minor importance when estimating the road grade. In the gearbox there are three types of efficiency losses: friction, viscous and a loss stemming from an oil pump in the gearbox. The friction coefficient,  $\mu_{gbx}$  is gear dependent and derived from measurements. The speed and gear dependency of the viscous loss is interpolated from measured curves. The loss from the oil pump is modelled as a constant. The model of the gearbox becomes:

$$\begin{aligned} T_{gbx.fric} &= T_{TC} \cdot i_{gbx}(gr) \cdot \mu_{fric}(gr) \\ T_{gbx} &= (T_{TC} - T_{gbx.pump}) \cdot i_{gbx}(gr) - \\ &|T_{gbx.visc}(\omega_{TC}, gr)| - |T_{gbx.fric}| \end{aligned} \quad (6)$$

$$\omega_{gbx} = \frac{\omega_{engine}}{i_{gbx}(gr)} \quad (7)$$

**Drop Box ( dbx ).** The dropbox is a gear box placed in the middle of the hauler translating the power downwards in the vehicles vertical direction and splitting it to the front axle and rear axles. Similar to the gearbox a friction loss and a viscous loss applies. Equation (8) to (9) displays the model of the drop box.

$$T_{dbx.fric} = (T_{gbx} \cdot i_{dbx} - |T_{dbx.visc}(\omega_{gbx})|) \cdot \mu_{fric} \quad (8)$$

$$\begin{aligned} T_{dbx} &= T_{gbx} \cdot i_{dbx} - |T_{dbx.visc}(\omega_{gbx})| - |T_{dbx.fric}| \\ \omega_{dbx} &= \frac{\omega_{gbx}}{i_{dbx}} \end{aligned} \quad (9)$$

**Centre Gear ( cgr ).** The denomination centre gear is used for the differential gear in the middle of

the axle. The centre gear is modelled as:

$$T_{cgr.fric} = T_{dbx} \cdot \mu_{fric} \quad (10)$$

$$\begin{aligned} T_{cgr} &= (T_{dbx} - |T_{cgr.fric}|) \cdot i_{cgr} - |T_{cgr.visc}| \\ \omega_{cgr} &= \frac{\omega_{dbx}}{i_{cgr}} \end{aligned} \quad (11)$$

**Hub Reduction ( hub ).** In the hub of the wheel a reduction gear and the brake is placed. The hub reduction gear is modelled according to the equations below.

$$T_{hub.fric} = T_{cgr} \cdot \mu_{fric} \quad (12)$$

$$\begin{aligned} T_{hub} &= (T_{cgr} - |T_{hub.fric}|) \cdot i_{hub} - |T_{hub.visc}(\omega_{cgr})| \\ \omega_{hub} &= \frac{\omega_{cgr}}{i_{hub}} \end{aligned} \quad (13)$$

**Wheel Brake ( brake ).**

The wheel brake is mounted in the hub. A speed dependent viscous loss applies to the brake independent if the wheel brakes are applied or not. If the wheel brakes are in operation the hydraulic brake pressure is measured and broadcasted via CAN. The wheel brake is modelled according to (14) to (16),

$$T_{brake} = P_{brake} \cdot A_{brakepiston} \cdot \mu_{brake}(\omega_{hub}) \cdot N_{fric.disc} \cdot r_{fric.disc} \quad (14)$$

$$\begin{aligned} T_{wheel} &= T_{hub} - |T_{brake.visc}(\omega_{hub})| - T_{brake} \\ \omega_{wheel} &= \omega_{hub} \end{aligned} \quad (15)$$

where  $P_{brake}$  = brake pressure,  $A_{brakepiston}$  = area of brake piston,  $\mu_{brake}$  = speed dependent brake disc friction coefficient,  $N_{fric.disc}$  = number of brake friction discs and  $r_{fric.disc}$  = average brake friction disc radius. A threshold is set to the brake pressure to avoid measurement ripple, thus, when  $P_{brake} \leq 200\text{kPa}$ ,  $T_{brake}$  is set to 0.

**Wheels ( Wheel ).** At the wheels the torque generated by the ICE and the applied brake force is translated into a traction (or retardation) force,  $F_t$ , see equation (17). At the wheels, the rotational inertia is also translated into a equivalent mass, equation (18),

$$F_t = \frac{T_{wheel}}{r_{wheel}} \quad (17)$$

$$\begin{aligned} m_{rot.TC} &= (J_{engine} + J_{TC} + J_{gbx-in}) \\ &\cdot (i_{gbx}(gr) \cdot i_{dbx} \cdot i_{cgr} \cdot i_{hub})^2 / r_{wheel}^2 \\ m_{rot.gbx} &= (J_{gbx-out} + J_{dbx-in}) \\ &\cdot (i_{dbx} \cdot i_{cgr} \cdot i_{hub})^2 / r_{wheel}^2 \end{aligned} \quad (18)$$

$$m_{rot.dbx} = (J_{dbx-out} + J_{cgr-in}) \cdot (i_{cgr} \cdot i_{hub})^2 / r_{wheel}^2$$

$$m_{rot.cgr} = (J_{cgr-out} + J_{hub-in}) \cdot (i_{hub})^2 / r_{wheel}^2$$

$$m_{rot.wheel} = (J_{hub-out} + J_{brake} + J_{wheel}) / r_{wheel}^2$$

where  $r_{wheel}$  is the radius of the wheel. The equivalent rotational mass is summarised with the vehicle mass,  $m_{veh}$ , to a total mass denominated  $m_{tot}$ .

$$\begin{aligned} m_{tot} &= m_{veh} + m_{rot.TC} + m_{rot.gbx} + m_{rot.dbx} \\ &+ m_{rot.cgr} + m_{rot.wheel} \end{aligned} \quad (19)$$

### 2.3 Complete Vehicle Model

Combining the drivetrain model, the external forces and Newton's second law of motion enables an expression for the longitudinal dynamics of the hauler. In continuous time the expression is:

$$m_{tot}(gr) \cdot \frac{d}{dt}v(t) = F_t(t) - F_a(t) - F_r(t) - F_g(t) \quad (20)$$

where  $gr$  = gear and  $t$  = time.

### 2.4 Model Alteration for Optimisation

The complete vehicle model is to a large extent reused when applied in the optimal control algorithm. Following the energy flow with the aim to calculate the engine speed and torque corresponding to a step in position and states, the structure of Section 2.1 to 2.3 is reused but in reversed order. When the ICE speed and torque is known it is translated into a fuel flow.

**Wheel Brake and Hub Reduction (torque/speed node cgr).** Differing from the wheel brake model in Section 2.2 there is no need to calculate the brake force when calculating the fuel cost. If the step in energy state (speed decrease) is negative and large enough so that application of the wheel brakes is necessary to achieve balance in equation (42), this will render in a loss of kinetic energy but since the ICE will operate without adding positive torque, no fuel will be injected and thus the fuel cost is 0.

**Torque Converter and Auxiliary Equipment (torque/speed node engine).** As the torque converter is modelled only to be operating in lock-up mode, the hauler never comes to full stop and consequently the energy state is always  $> 0$  in the optimised speed trajectory. In practise this has limited impact since the very high combined gear ratio in a hauler enables very low vehicle speeds and since it is only at the end of the cycle  $v = 0$  is desired. At the engine speed/torque node the loss from the ICE's auxiliary equipment (alternator, fan, etc) is added by means of a look-up table, equation (21). This is not necessary when the model is used for road estimation since the measured torque signal from the engine ECU includes the auxiliary equipment loss.

$$T_{Engine} = T_{TC} + T_{aux.equip}(\omega_{TC}) \quad (21)$$

**Internal Combustion Engine (ICE).** The internal combustion engine model in the optimisation algorithm consists of a measured look up table with engine speed,  $\omega_{Engine}$ , and engine torque,  $T_{Engine}$  as input and the fuel mass flow,  $\dot{m}_f$  as output. The cost in fuel mass,  $m_f$  [kg], for one step in distance with corresponding changes of states is evaluated using equation (45).

## 3 ESTIMATION OF ROAD INCLINATION AND ROLLING RESISTANCE

Section 3 outlines a method for collecting the road related data that is needed in the optimisation algorithm. The intention is to use sensors available in a standard articulated hauler complemented with a commercially available GPS. The data is collected and processed in a Matlab algorithm and the road is stored in a map like format with latitude and longitude coordinates as identification points. The main parameters that are identified in the algorithm are: latitude ( $\phi$ ), longitude ( $\lambda$ ), altitude ( $z$ ), mean vehicle speed ( $v$ ), road inclination ( $\alpha$ ), vehicle heading ( $\beta$ ), rolling resistance coefficient ( $c_r$ ), speed limit ( $v_{max}$ ) and travelling direction (Dir.). Of the quantities stored in the map, only  $\phi, \lambda, \alpha, c_r$  and  $v_{max}$  are used in the optimisation algorithm presented in Section 4. A method to estimate the road inclination for on-road commercial vehicles is exhaustively described in (Sahlholm, 2011) and has been further enhanced for off-road vehicles and to include rolling resistance in the work of (Almesåker, 2010) and (Saaf and Hana, 2011). The method used utilizes an extended Kalman filter (EKF) to work as an observer for the unmeasured parameter rolling resistance and also to help removing potential bias error that develops when only using an inclination sensor to measure the road inclination (Sahlholm, 2011), p.80-88. In the estimation model, Section 3.2.6, the vehicle model described in Section 2 and the road model described in Section 3.2.5 are combined to generate the quantities stored in the road map.

### 3.1 Map Building Process

The intention with the proposed map building process is that the operator initially travels the track between the loading and unloading sites 2 times to initiate the map. The map data is updated off-line after each finished run which is a feasible scenario on a construction site since the distance between the loading and unloading sites normally are within 2 km (approx. 6 min travel). On a high level, the map building process can be described according to the steps below:

1. Operator drives the track between the loading and unloading site forth and back as fast (but safe) as possible while necessary sensor data is recorded.
2. The direction of the travel is detected and the data updated accordingly.
3. The collected data is processed in the map-building algorithm according to:
  - (a) Calculation of applied brake force.

- (b) Translation of ICE torque into force at wheels.
  - (c) Geographic and vehicle dependent data (measured and calculated) are merged in an Extended Kalman Filter (EKF).
  - (d) Smoothing of estimates with Rauch-Tung-Striebel algorithm to remove potential lag.
  - (e) Merge the estimates into a map utilising a fusion algorithm.
4. The highest recorded speed at each coordinate is used to set the max speed limit.

As additional runs are travelled during production new data is merged into the map after each run, improving the quality of the map.

### 3.2 Sensor and Data Fusion

The proposed map building algorithm utilises data recorded from an external GPS:  $\varphi, \lambda, z, \beta$  and the vehicle CAN:  $v, \alpha$ , vehicle articulation ( $\Phi$ ), engine torque ( $T_{engine}$ ). The GPS sensor used in the tests was a Garmin GPS18x OEM. The accuracy according to the manufacturer (Garmin international inc., 2011) is for position:  $< 15m$ , 95 % typical and for velocity: 0.1 knot RMS steady state in GPS Standard Positioning Service mode and position:  $< 3m$ , 95 % typical and velocity: 0.1 knot RMS steady state in WAAS mode. No specific data on the accuracy of the altitude signal is given.

#### 3.2.1 Time vs Spatial Sampling

The predominant way to describe a road is through map coordinates. Using distance rather than time as the independent variable facilitates the fusion of data from several different runs along the road since different runs may have been travelled in opposing direction and at different speeds. To shift to distance as the independent variable the following conversion is used in the vehicle's longitudinal model.

$$\frac{dv}{dt} = \frac{dv}{ds} \frac{ds}{dt} = v \frac{dv}{ds} \Rightarrow \frac{dv}{ds} = \frac{1}{v} \frac{dv}{dt}, v \neq 0 \quad (22)$$

#### 3.2.2 Sensor Fusion

Several different methods for sensor fusion are available, see e.g. (Gustafsson, 2012). The Kalman filter and the extended Kalman filter (EKF) are well-known mathematical methods for sensor fusion that also enables the possibility to estimate the states of a process. This is a valuable feature since the rolling resistance is not directly measurable with the standard mounted sensors on an articulated hauler. While the Kalman filter method only are able to estimate the

states of a linear process the extended Kalman filter method gives the possibility to estimate the states in a non-linear process (Welch and Bishop, 2006). Based on the findings in (Sahlholm, 2011) and (Almesåker, 2010) the extended Kalman filter was chosen as the method for sensor fusion in the map building process. The use of the extended Kalman filter in the proposed map building process follows to a large extent the guidance given in (Welch and Bishop, 2006).

#### 3.2.3 Smoothing

To compensate for filtering delay and to include later measurements in the estimate for each data point a smoother is applied after each run. The Rauch-Tung-Striebel (RTS) smoother (Rauch et al., 1965) is an efficient two-pass algorithm for fixed interval smoothing. The use of the RTS smoother is possible since the intention is to update the map only after a complete run along the road.

#### 3.2.4 Data Fusion

A general data fusion method is used to merge data from different runs along the road. The data fusion method is described in (Gustafsson, 2012), p.30. After the data has been merged, the data is stored in the map for each coordinate pair along with the covariance matrix.

#### 3.2.5 Road Model

In the proposed road model the identification points are separated with a nominal distance  $\Delta s$ , as described in Section 3.2.7. Out of the 7 appended road parameters only the correlation between road altitude,  $z$ , and road inclination angle,  $\alpha$ , is modelled as the other parameters are either measured or observed in the Kalman filter. The correlation between road altitude and road inclination angle is modelled as

$$\frac{dz}{ds} = \sin(\alpha(s)) \quad (23)$$

#### 3.2.6 Estimation Model

This section describes how the road parameter estimation is made and the models used in the estimation process.

**Extended Kalman Filter ( EKF ) and Smoothing.** The states to be estimated presented in continuous time are displayed in (24).

$$\hat{x}(t) = [\varphi(t) \lambda(t) z(t) v(t) \alpha(t) \beta(t) c_r(t)]^T \quad (24)$$

The explanation of the parameters are found in the beginning of this section. As described in 3.2.1 spatial samples are used instead of continuous time in the model. To shift to distance as the independent variable equation (22) is used. Equation (24) is translated into discrete notation, see equation (25), where k represents the index of the location.

$$\hat{x}_k = [\varphi_k \lambda_k z_k v_k \alpha_k \beta_k c_{r,k}]^T \quad (25)$$

Time update (a priori estimate).

1. Define two distances, one in meters and one in degrees:

$$\begin{aligned} \Delta s_{m,k} &= \hat{v}_k \cdot T_s \\ \Delta s_{deg,k} &= \frac{\Delta s_{m,k}}{r_{earth}} \cdot \frac{180}{\pi} \end{aligned} \quad (26)$$

2. Project the state ahead (state equations).

$$\hat{x}_k^- = \begin{bmatrix} \varphi_{k-1} + \Delta s_{deg,k-1} \cos(\alpha_{k-1}) \cos(\beta_{k-1}) \\ \lambda_{k-1} + \Delta s_{deg,k-1} \cos(\alpha_{k-1}) \sin(\beta_{k-1}) \\ z_{k-1} + \Delta s_{m,k-1} \sin(\alpha_{k-1}) \\ v_{k-1} + \frac{\Delta s_{m,k-1}}{v_{k-1}} \frac{F_{t,k-1} - F_{a,k-1} - F_{g,k-1} - F_{r,k-1}}{m_{tot}} \\ \alpha_{k-1} \\ \beta_{k-1} + \Delta s_{m,k-1} \frac{\cos(\alpha_{k-1})}{r_{turn,k-1}} \\ c_{r,k-1} \end{bmatrix} \quad (27)$$

With:

$$r_{turn,k-1} = l_1 \cot(\Phi_{k-1}) + \frac{l_2}{\sin(\Phi_{k-1})} \quad (28)$$

where  $r_{turn}$  is the turning radius of the vehicle,  $\Phi$  is the articulation angle,  $l_1$  and  $l_2$  distances between axles and articulation point (front / rear).

3. Project the error covariance ahead

Define the Jacobian:  $A[i,j] = df[i]/dx[j]$  and project the error covariance:

$$P_k^- = A \cdot P_{k-1} \cdot A^T + Q \quad (29)$$

4. Measurement update (a priori estimate) Define the measurement vector:

$$y_k = [\varphi_{k.gps} \lambda_{k.gps} z_{k.gps} v_{k.CAN} \alpha_{k.CAN} \beta_{k.gps}]^T \quad (30)$$

Measurement equation:

$$y_k = H \cdot x_k + e_k \quad (31)$$

where the H matrix is:

$$H = [ I_6 \quad h_{*7} = 0 ] \quad (32)$$

Calculate the Kalman gain:

$$K_k = P_k^- H^T (H P_k^- H^T + R)^{-1} \quad (33)$$

5. Update estimates with measurement

$$\hat{x}_k = \hat{x}_k^- + K_k (y_k - H \hat{x}_k^-) \quad (34)$$

6. Update error covariance

$$P_k = (I - K_k H) P_k^- \quad (35)$$

7. Save  $\hat{x}_k$ ,  $P_k$ ,  $\hat{x}_k^-$  and  $P_k^-$  at each coordinate [k] to be used in smoothing process.

8. Initiate smoothing with the last predicted values ( $\hat{x}_{N+1|N}^-$ ) and last predicted covariance matrix ( $P_{N+1|N}^-$ ), where N is the total number of measured data points. Run smoothing backwards along the track. Kalman smoothing gain:

$$K_k^s = P_{k|k} + A^T P_{k+1|k}^{-1} \quad (36)$$

Smoothed estimates:

$$\hat{x}_{k|N}^s = \hat{x}_{k|k} + K_k^s (\hat{x}_{k+1|N}^s - \hat{x}_{k+1|k}^-) \quad (37)$$

Smoothed error covariance matrix

$$P_{k|N}^s = P_{k|k} (P_{k+1|N}^s - P_{k+1|k}^-) K_k^{sT} \quad (38)$$

### 3.2.7 Fusion of Map Data

A reference track is chosen and split into 6m long sections. The knot points are identified through the  $\varphi$  and  $\lambda$  coordinates and the corresponding states are appended. When the reference map is compared with a recorded track the search area of new measurements is limited to points which have the same heading,  $|\beta| \leq 15^\circ$  and to a rectangular area that is  $\pm 1.5m$  in the heading direction and  $\pm 8m$  orthogonal to the heading. If driven in reversed direction, the sign of  $\alpha$  and the heading is switched (180 deg). Out of the points in the new track that is in the search area, the point that is closest to the reference point in the horizontal plane is chosen. The tracks are merged into the stored map through fusion of independent estimates as described in (Gustafsson, 2012), p.30. The states in the map is calculated according to equation (39).

$$\begin{aligned} P_k^f &= ((P_k^1)^{-1} + (P_k^2)^{-1})^{-1} \\ \hat{x}_k^f &= P_k^f \cdot ((P_k^1)^{-1} \hat{x}_k^1 + (P_k^2)^{-1} \hat{x}_k^2) \end{aligned} \quad (39)$$

## 4 OPTIMAL CONTROL OF AN ARTICULATED HAULER

In this section a method to control the velocity and gear shift of an articulated hauler as it travels along a road with varying inclination and surface conditions is developed. The target is to derive a Pareto front of minimum fuel consumption vs cycle time. Input to the optimisation algorithm is machine data and the road dependent data developed in Section 3.

## 4.1 Objective

The objective is to transport material at a set production rate [ton/hour], which easily translates into cycle time, while minimising fuel consumption. A Pareto front is built through running the optimisation procedure a number of times with different cycle time targets achieving a set of discrete cycle time - min fuel consumption points. Denominating each individual optimisation procedure with  $i$ , the objective becomes:

$$\begin{aligned} &\text{minimise } M_i \quad i = 1, \dots, n && (P1) \\ &\text{s.t. } t_i \end{aligned}$$

where  $M_i$  = fuel consumption in cycle  $i$  and  $t_i$  = cycle time in cycle  $i$ . Dynamic programming is used as method for the optimisation and to avoid the *Curse of dimensionality* ((Bellman, 1961)) the approach of (Monastyrsky and Golownykh, 1993) and (Hellström et al., 2010) is used, i.e. the trip time is added to the criteria in (P1) which becomes:

$$\text{minimise } M_i + \beta_i t \quad i = 1, \dots, n \quad (P2)$$

The trade-off between fuel consumption and cycle time is represented by the scalar coefficient  $\beta$ . The  $n$  number of discrete points in the Pareto front is established through varying  $\beta$   $n$  times. The lower limit of the cycle time in the Pareto front is found through setting  $\beta$  high enough to reach maximum speed limit and the upper limit is found through setting  $\beta$  low enough so no further fuel consumption decrease is found.

## 4.2 Dynamic Programming

Dynamic Programming (DP), developed in the 1950's by Richard Bellman, is a well known algorithm to solve optimal control problems. Considering road topology and rolling resistance as a priori known disturbances (by means of the earlier described map-module) and since dimension is small, DP suits the optimal control problem at hand well. While the DP algorithm is not described in-depth here, the reader is referred to (Bellman and Dreyfus, 1962) and e.g. (Guzzella and Sciarretta, 2013).

### 4.2.1 State Space

While it is the cycle time / fuel consumption trade off that is the main objective a natural choice for the first state variable would be vehicle speed. However, following the findings in (Hellström et al., 2010), having energy as the state variable damps the oscillatory behaviour of the control while using the preferred Euler forward method for discretisation. Thus, energy is chosen as the first state variable. The second state variable is gear number rendering in the state vector:  $x_k = [e_k \text{ } gr_k]^T$ , where  $e$  = energy and

$gr$  = gear number. Denominating the control variables  $u$ , the control vector is  $u_k = [u_{e,k} \text{ } u_{gr,k}]^T = [e_{k+1} - e_k \text{ } gr_{k+1} - gr_k]^T$ .

### 4.2.2 Control Constraints

Since the proposed drivetrain model is limited to lock-up mode, see Section 2.4, a min limit for the velocity needs to be set. The max limit of the speed is an input to the optimisation procedure from the map module. Consequently the vehicle speed is limited to

$$v_{min} \leq v \leq v_{max} \quad (40)$$

Due to limitations in the gearbox a limit on gear steps is introduced i.e. the maximal number of gear shifts is 2 (both up and down shift).

$$gr_k - 2 \leq gr_{k+1} \leq gr_k + 2 \quad (41)$$

## 4.3 Dynamic Model

The vehicle model in Section 2, with alterations described in Section 2.4, is used. Thus the complete vehicle model is the same as in equation (20). Translated into spatial coordinates and reformulated into terms of energy (20) becomes:

$$\frac{de}{ds} = F_t - F_a - F_r - F_g \quad (42)$$

## 4.4 Discretisation

The optimisation problem is solved numerically and must be discretised. The data from the map module is discrete and split into  $N$  steps of length  $h$  such that the total distance of the transport mission,  $S$ , equals

$$S = \sum_{k=1}^N h_k \quad (43)$$

Utilising Euler forward method to discretise equation (42), the discretised complete vehicle model is written

$$\frac{e_{k+1} - e_k}{h_k} = F_{t,k} - F_{a,k} - F_{r,k} - F_{g,k} \quad (44)$$

Similarly the fuel mass flow  $\dot{m}_f$  is transformed into spatial representation using equation (22) and then discretised with the Euler method.

$$m_{f,k+1} = m_{f,k} + \frac{h_k}{v_k} \dot{m}_{f,k} \quad (45)$$

## 4.5 Cost Function

The cost function is a central part of the DP algorithm and in the work at hand based on calculating the equivalent fuel cost,  $m_f$ , for bringing the vehicle from one position on the road to the next position. During the transition both states, i.e. the kinetic energy (speed) and the gear, may change. A time penalty, introduced in Section 4.1 and the cost for changing gear described below, are added to the cost function.

$$\zeta = m_f + \beta t + m_{f.gs} \quad (46)$$

Differing from the drivetrain model in the map module, see 2.2, the efficiency loss in the gearbox at gear shifts is accounted for in the optimisation algorithm. The cost of a gear shift is approximately equal to the work that is lost speeding up or slowing down the engine to meet the next gear. In the model, this is implemented as the fuel flow needed to accelerate or decelerate the engine inertia plus the inertia of components up to the point where the gear is engaged. The fuel flow is multiplied with the time of the gear shift resulting in a fuel mass penalty,  $m_{f.gs}$ .

$$\dot{\omega}_{gs} = \left| \frac{(\omega_{engine.k}(gr) - \omega_{engine.k+1}(gr))}{I_{gs}} \right| \quad (47)$$

$$T_{gs} = \dot{\omega}_{gs} * J \quad (48)$$

$$m_{f.gs} = \dot{m}_{f.gs}(\omega_{engine.k}, T_{gs}) \cdot I_{gs} \quad (49)$$

## 5 RESULT

To test the map module a 1.2km long gravel road was travelled with an articulated hauler 3 times in each direction while needed sensor data was recorded. The data was processed off-line in a Matlab script designed according to the method described in Section 3. A comparison between measured / estimated parameters and the resulting fused data stored in the map is shown in Figure 4 to 7. As seen in Figure 4 and 5 the latitude - longitude and especially the altitude signal from the GPS have rather poor accuracy. In the vertical plane the spread in the GPS signal is approximately 10m. Also the signal from the road angle sensor is wildly fluctuating in real working condition. Except for the endpoints of the track, the use of sensor fusion and fusion of data from several runs averages the spread in the individual measurements to make a uniform estimation of the road. At the endpoints of the track (i.e. the loading/unloading area) there is much larger spread in the hauler's movements (position, speed, heading, articulation etc.) and the method has some difficulties in finding reference

measurements rendering in some unexpected fluctuation in the stored map. A solution to this would be to define a loading respectively unloading area, e.g. implemented as a circle, and then only store map data between the periphery of the two circles.

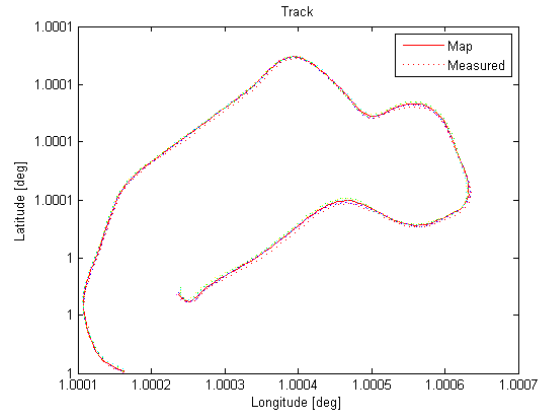


Figure 4: Measured and resulting latitude and longitude coordinates stored in the map. (axes normalised)

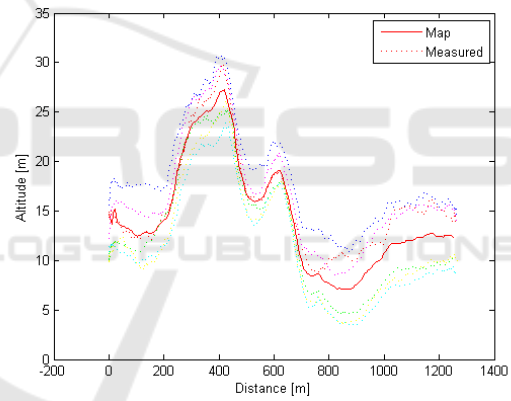


Figure 5: Measured and resulting altitude stored in the map.

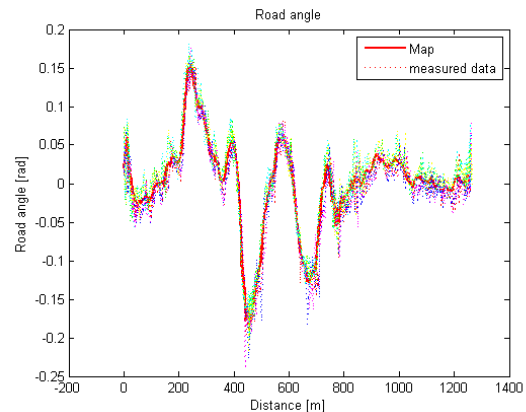


Figure 6: Measured and resulting road angle stored in the map.

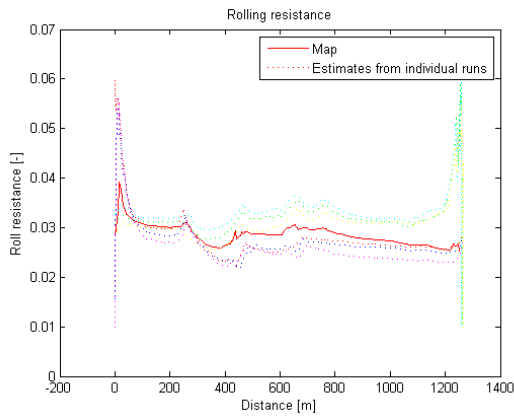


Figure 7: Individual estimations and fused rolling resistance stored in the map.

A test to see how well the method estimates the rolling resistance was performed. Since it is very difficult to measure the rolling resistance of an articulated hauler in actual working conditions, the measured GPS data was combined with a pre-set rolling resistance,  $c_r = 3\%$ , and then the hauler drive was simulated with a Volvo in-house developed software to generate the engine torque and speed signals needed in the map module. The map module was run on the created data and a comparison of the estimated rolling resistance and the pre-set is shown in Figure 8. Even if only one drive is used as input, due to difficulties in syncing measured and simulated data, (the estimation is enhanced if several turns are driven) the rolling resistance is well represented after some initialisation time.

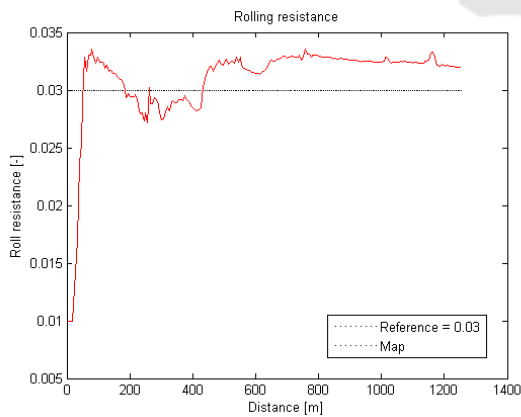


Figure 8: Verification of rolling resistance estimation.

Utilising the created map as input to the optimal control module a speed and gear shift optimisation can be performed. Figure 9 to 10 displays optimal speed and gear-shift trajectories when the time penalty is set to  $\beta = 0.007g/s$ . In the figures a comparison is made to speed and gear trajectories as sim-

ulated with an in-house Volvo tool when the speed is limited to 30/km/h which gives a similar cycle time.

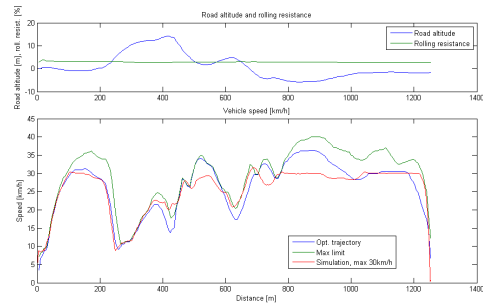


Figure 9: Vehicle speed trajectory.

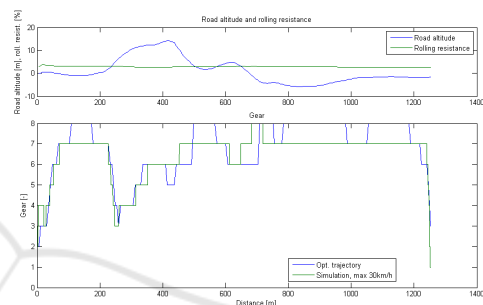


Figure 10: Gear trajectory.

As seen in Figure 9 in the optimal trajectory the hauler picks-up speed in the down slopes generating kinetic energy which is utilised when the road goes up. Figure 10 shows that when the gear shift is optimised higher gear is consistently used enabling lower engine speeds and reducing fuel consumption. The combination of optimal speed and gear saves approx. 9 % fuel compared to when a fixed target speed is set. The comparison of how the fuel consumption develops along the track is shown in Figure 11.

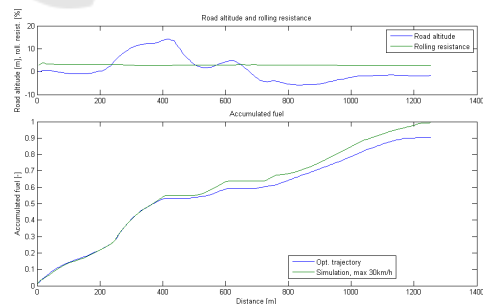


Figure 11: Accumulated fuel consumption (normalised).

Following the method described in Section 4.1 a Pareto front trading fuel consumption against cycle time is built, see Figure 12. The graph shows a clear increase in fuel consumption if the cycle time is decreased below approx. 200s.

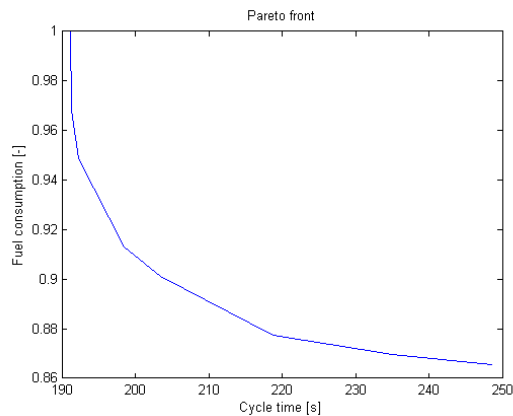


Figure 12: Pareto front showing trade-off (normalised) fuel consumption vs cycle time.

## 6 CONCLUSION

A method to generate a map which includes parameters important for optimisation in off-road conditions, such as road inclination and rolling resistance, has been developed. The method utilises sensors mounted as standard on a Volvo articulated hauler combined with a commercially available GPS sensor. The main algorithms used is an extended Kalman filter to merge sensors, a RTS smoother to remove the filter lag and a data fusion algorithm to merge data from several runs along the road. The map is used as input to the optimal control problem to minimise fuel consumption in a articulated hauler transport mission towards a set cycle time. A Dynamic Programming algorithm is developed to solve the optimal control problem. In the DP algorithm, optimal vehicle speed and gear shift trajectories are computed enabling the hauler to make best use of its kinetic energy and to consistently choose high gears to enable low engine speed, minimising fuel consumption. In the test case, a potential reduction of fuel consumption of up to 9%, verified by computer simulations, is shown when compared to a simulation of the same transport mission where a fixed mean speed target is used to achieve an equal cycle time. The proposed optimisation method is utilised to create a Pareto front of fuel consumption vs cycle time for the transport mission, which can be used for the hauler transport itself or when solving a larger optimal control problem involving several construction machines working together on a transport mission. Different means to get the articulated hauler to follow the optimal control trajectories are plausible. One is to implement a human machine interface (HMI) instructing the driver to follow the optimal speed trajectory, a second could be to design a cruise control software that controls speed and gear

shifts (under the operators supervision) and in an autonomous hauler the system could be integrated into the control system of the machine.

## ACKNOWLEDGEMENTS

This research is supported by FFI - Strategic Vehicle Research and Innovation.

## REFERENCES

- 21st Century truck partnership (2013). 21st century truck partnership and technical white papers. [www.energy.gov/sites/prod/files/2014/02/f8/21ctp\\_roadmap\\_white\\_papers\\_2013.pdf](http://www.energy.gov/sites/prod/files/2014/02/f8/21ctp_roadmap_white_papers_2013.pdf).
- Almesåker, B. (2010). Iterative map building for gear shift decision. Master's thesis, Uppsala University.
- Bellman, R. (1961). *Adaptive control process*. Princeton University Press.
- Bellman, R. E. and Dreyfus, S. E. (1962). *Applied dynamic programming*. Princeton University Press.
- Fu, J. and Bortolin, G. (2012). Gear shift optimization for off-road construction vehicles. In *Procedia - social and behavioral science*, volume 54. SCIENCEDIRECT.
- Garmin international inc. (2011). Gps 18x technical specifications. [http://static.garmin.com/pumac/GPS\\_18x\\_Tech\\_Specs.pdf](http://static.garmin.com/pumac/GPS_18x_Tech_Specs.pdf).
- Gustafsson, F. (2012). *Statistical sensor fusion*. Studentlitteratur AB, 2:1 edition.
- Guzzella, L. and Sciarretta, A. (2013). *Vehicle propulsion systems*. Springer-Verlag, 3 edition.
- Hellström, E., Åslund, J., and Nielsen, L. (2010). Design of an efficient algorithm for fuel-optimal look-ahead control. *Control Engineering Practice*, 18(11):1318–1327.
- Monastyrsky, V. V. and Golownykh, I. M. (1993). Rapid computations of optimal control for vehicles. *Transportation Research*, 27B(3):219–227.
- Rauch, H. E., Striebel, C. T., and Tung, F. (1965). Maximum likelihood estimates of linear dynamic systems. *AIAA Journal*, 3(8):1445–1450.
- Saaf, M. and Hana, A. (2011). Map building and gear shift optimization for articulated haulers. Master's thesis, Mälardalen University.
- Sahlholm, P. (2011). *Distributed road grade estimation for heavy duty vehicles*. PhD thesis, Royal Institute of Technology, Stockholm.
- Welch, G. and Bishop, G. (2006). An introduction to the kalman filter. Technical report, University of North Carolina at Chapel Hill.